Spinor Bose-Einstein condensates in a double well: Population transfer and Josephson oscillations

B. Juliá-Díaz, M. Melé-Messeguer, M. Guilleumas, and A. Polls
Departament d'Estructura i Constituents de la Matèria, Universitat de Barcelona, 08028 Barcelona, Spain
(Received 17 July 2009; published 26 October 2009)

The dynamics of an $F=1$ spinor condensate in a two-well potential is studied within the framework of the Gross-Pitaevskii equation. We derive two-mode equations relating the population imbalances, the phase differences among the condensates at each side of the barrier and the time evolution of the different Zeeman populations for the case of small population imbalances. The case of zero total magnetization is scrutinized in this limit demonstrating the ability of a two-mode analysis to describe to a large extent the dynamics observed in the Gross-Pitaevskii equations. It is also demonstrated that the time evolution of the different total populations fully decouples from the Josephson tunneling phenomena. All the relevant time scales are clearly identified with microscopic properties of the atom-atom interactions.

DOI: 10.1103/PhysRevA.80.043622 PACS number(s): 03.75.Mn, 03.75.Lm

The recent experimental work on optically trapped spinor condensates has broadened the frontiers of confined Bose-Einstein condensates (BECs) [1,2]. There, a transfer of population between the different Zeeman components of a spinor BEC was observed providing a clear signal of the spin-dependent interatomic interactions. This experiment quickly connected the field of cold atoms to a large variety of problems in quantum magnetism, mostly related to magnetic ordering and spin dynamics [3]. From a different point of view, it can be regarded as the first case of ternary mixture of BECs with population exchange among the three components, a nice example of coupled multicomponent quantum gases.

At the same time, the fast tunneling of atoms through potential barriers driven by imbalanced populations at each side of the barrier was shown experimentally, short after it was observed in optical lattices [4], providing the first confirmation of Josephson tunneling of atoms in BECs [5]. From the BEC point of view, Josephson tunneling through the potential barrier produces a weak coupling between the BECs at each side of the trap, presenting a coupled-oscillator behavior in the appropriate variables [6].

Both effects have been considered by several theoretical groups in quite different contexts, e.g., [6–12]. In this paper we address both aspects together: the Josephson oscillations and the transfer of populations. Providing a direct connection between the different time scales and the microscopic properties of the interatomic interactions.

To fix the conditions we consider the simplest scenario, which already contains relevant physics. We restrict our analysis to the case of small population imbalance of all the Zeeman sublevels and small initial phase difference between the same component at both sides of the trap. Our main tool is the mean-field Gross-Pitaevskii (GP) equations for spinor BECs [10]. On top of numerical solutions to the GP equations we illustrate the physics emerging in this fairly complex situation by deriving a two-mode description of the problem. Within this two-mode description it is easy to show that for small population imbalances and phase differences the population transfer dynamics fully decouples from the tunneling phenomena.

In the mean-field approximation the dynamics of the vector order parameter $\Psi=(\Psi_{-1},\Psi_0,\Psi_1)$ representing the $F=1$ spinor condensate is given by [10]

$$\imath\hbar\partial_t\Psi_{\pm1}=[\mathcal{H}_s+c_2(n_{\pm1}+n_0-n_{\mp1})]\Psi_{\pm1}+c_2\Psi_0^2\Psi_{\mp1}^*$$

$$\imath\hbar\partial_t\Psi_0=[\mathcal{H}_s+c_2(n_1+n_{-1})]\Psi_0+c_2 2\Psi_1\Psi_0^*\Psi_{-1}, \quad (1)$$

where, $\mathcal{H}_s=-\frac{\hbar^2}{2M}\nabla^2+V+c_0n$, $n_m(\vec{r},t)=|\Psi_m(\vec{r},t)|^2$, $n(\vec{r},t)=\Sigma_m n_m(\vec{r},t)$, and $m=0,\pm1$. The population of each hyperfine sublevel is $N_m(t)=\int d\vec{r}n_m(\vec{r},t)$. Due to the last term in the r.h.s of Eq. (1), the population of each Zeeman sublevel is not conserved. The couplings are $c_0=4\pi\hbar^2(a_0+2a_2)/(3M)$ and $c_2=4\pi\hbar^2(a_2-a_0)/(3M)$, where a_0 and a_2 are the scattering lengths describing binary elastic collisions in the channels of total spin 0 and 2, respectively. Their values for ^{87}Rb are $a_0=101.8a_B$ and $a_2=100.4a_B$ [13], which yield $c_2<0$, thus producing a ferromagnetic-like behavior. The total number of atoms in the system and total magnetization are conserved quantities, $N=\int d\vec{r}n(\vec{r},t)$ and $M=\int d\vec{r}[n_{+1}(\vec{r},t)-n_{-1}(\vec{r},t)]$.

We consider a setup similar to that described in Ref. [5] but with two important differences: the total number of atoms and the barrier height. In our case the number of atoms is larger, $N=15\,000$, in order to enhance population transfer effects. We use the same kind of double-well potential but with a higher barrier and a tighter confinement in the x direction to ensure a clear Josephson tunneling situation. The potential then reads as

$$V(\vec{r})=\frac{M}{2}(\omega_x^2x^2+\omega_y^2y^2+\omega_z^2z^2)+V_0\cos^2(\pi x/q_0)$$

with $\omega_x=2\pi\times100$ Hz, $\omega_y=2\pi\times66$ Hz, $\omega_z=2\pi\times90$ Hz, $q_0=5.2$ μm, $V_0=3500h$ Hz, and M is the mass of the atoms. As in the experiment [5] we assume that the dynamics takes place essentially on the x axis. Then, defining $\omega_\perp=\sqrt{\omega_z\omega_y}$ the coupling constants can be rescaled by a factor $1/(2\pi a_\perp^2)$, with $a_\perp$ the transverse oscillator length [14], and the dynamical equations transform to one-dimensional ones for a symmetric double well.

The numerical simulations of Eqs. (1) are performed in the following way. First using an imaginary time evolution method we compute the ground, $\Phi_{GS}\equiv\Phi_+$, and first-excited state, $\Phi_{1st}\equiv\Phi_-$ of a scalar BEC, $c_2=0$, under the same

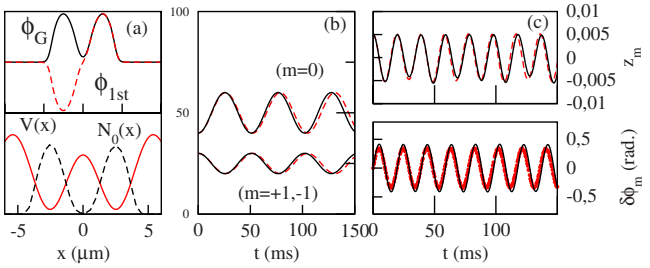

FIG. 1. (Color online) (a) (above) Φ_G and Φ_{1st}. (below) Potential in the x direction together with one of the initial population profiles used in the simulations (arbitrary units). The solid (black) curves show the evolution of the total population (b) and of the population imbalances and phase differences (c) corresponding to simulation I of Table I. The dashed (red) lines depict the two-mode calculation.

conditions. Then, given initial population imbalances for all the components, we build $t=0$ wave functions by the appropriate linear combinations of Φ_+ and Φ_-. We study the time evolution of the system by means of the split operator method. In Fig. 1 we depict Φ_{GS}, Φ_{1st} and the potential in the x direction together with one of the initial density profiles used in the simulations.

To characterize the Josephson dynamics we define for each component the population imbalance, $z_m=(N_{m,L}-N_{m,R})/N_m$, and the phase difference, $\delta\phi_m=\phi_{m,R}-\phi_{m,L}$. Where, $N_{m,L}(t)=\int_{-\infty}^{0}dx\int_{-\infty}^{\infty}\int_{-\infty}^{\infty}dydzn_m(\vec{r},t)$, $N_{m,R}(t)=N_m(t)-N_{m,L}(t)$ and $\phi_{m,R(L)}$ are the space average of the phase of $\Psi_m(\vec{r},t)$ at each side of the barrier. Let us emphasize that the phase of $\Psi_m(\vec{r},t)$ is almost spatially constant at each side of the trap during the GP simulations.

To better understand the dynamical content of the GP results, Eq. (1), we derive a two-mode approximation for the GP description of spinor BEC based on the following ansatz, $\Psi_m(\vec{r},t)=\Psi_{m,L}(t)\Phi_{m,L}(\vec{r})+\Psi_{m,R}(t)\Phi_{m,R}(\vec{r})$, where the modes $\Phi_{m,L(R)}$ are mostly localized at the left (right) side of the trap. These modes can be built from $\Phi_\pm$ obtained from the GP equations, $\Phi_{m,L}=\frac{1}{\sqrt{2}}(\Phi_{m,+}+\Phi_{m,-})$, $\Phi_{m,R}=\frac{1}{\sqrt{2}}(\Phi_{m,+}-\Phi_{m,-})$ with $\Phi_{m,\pm}(\vec{r})=\pm\Phi_{m,\pm}(-\vec{r})$. The complex components are normalized as, $\Psi_{m,L}=\sqrt{N_{m,L}(t)}e^{i\phi_{m,L}}$ and $\Psi_{m,R}=\sqrt{N_{m,R}(t)}e^{i\phi_{m,R}}$. Therefore, for this case, $z_m=(N_{m,L}-N_{m,R})/N_m$, and $\delta\phi_m=\phi_{m,R}-\phi_{m,L}\ \forall\ m$.

As a first step we consider the so-called standard two-mode, which implies that all the overlapping integrals involving products of L and R modes of any two components are neglected. This approximation is expected to yield essentially the correct physics as it was for the case of the scalar condensate or binary mixtures [9,15].

We take the following assumptions: zero total magnetization, small imbalances, z_m, small phase differences, $\delta\phi_m$, and small $\delta\phi_{L(R)}\equiv 2\phi_{0,L(R)}-\phi_{+1,L(R)}-\phi_{-1,L(R)}$. Also we take equal modes for the three states ($\Phi_{L(R)}\equiv\Phi_{m,L(R)}\ \forall\ m$), which is fully justified at zero magnetic field (it corresponds to the single mode approximation at each well).

In such conditions one can prove that the total population of the different components, $N_m(t)$, fully decouples from the Josephson tunneling dynamics. The time evolution of N_0 is given by,

$$\ddot{N}_0(t)=-4U_2^2N_0(t)[N-N_0(t)][N_0(t)-N/2], \tag{2}$$

with $\hbar U_2=c_2\int d\vec{r}\phi_{L(R)}^4(\vec{r})$, where one can indistinctly use the left or the right mode. The other two follow: $N_{\pm1}(t)=[N-N_0(t)]/2$. If $N_0(t)\sim N/2$, the behavior of N_0 becomes sinusoidal, $N_0(t)=N/2+[N_0(0)-N/2]\cos(\omega_T t)$, where we have defined the "population transfer frequency," $\omega_T=NU_2$. Equation (2) gives an excellent agreement compared to the full GP results. With the considered conditions no damping is observed in the evolution of the populations.

The system of equations governing the dynamics of the population imbalances, z_m, and phase differences, $\delta\phi_m$, reads as

$$\dot{z}_{\pm1}=-\omega_r\delta\phi_{\pm1}-(N_0/2)U_2(\delta\phi+z_{\pm1}\Delta\phi),$$

$$\dot{z}_0=-\omega_r\delta\phi_0+\bar{N}U_2(\delta\phi+z_0\Delta\phi),$$

$$\delta\dot{\phi}_{\pm1}=U(\bar{N}z_{\pm1}+N_0z_0)+U'\bar{N}z_{\mp1}+\omega_r z_{\pm1}+U_2\frac{N_0}{2}(2z_0-z_{\pm1}+z_{\mp1}),$$

$$\delta\dot{\phi}_0=(U+U_2)\bar{N}(z_{-1}+z_{+1})+U_0N_0z_0+\omega_r z_0$$

$$\Delta\dot{\phi}=8(N_0-N/2)U_2, \tag{3}$$

where $\delta\phi=\delta\phi_L-\delta\phi_R$, $\Delta\phi=\delta\phi_L+\delta\phi_R$, $\bar{N}\equiv N_{+1}=N_{-1}=(N-N_0)/2$, $\hbar U_0=c_0\int d\vec{r}\phi_{L(R)}^4(\vec{r})$, $U=U_0+U_2$, $U'=U_0-U_2$, $K=-\int d\vec{r}[\hbar^2/(2M)\vec{\nabla}\Phi_L\cdot\vec{\nabla}\Phi_R+\Phi_L V\Phi_R]$, and $\omega_r=2K/\hbar$, is the Rabi frequency.

From the ground and first-excited states of the system computed numerically, see Fig. 1, we build the left and right modes as explained above and compute the microscopic parameters entering in the two-mode description. The resulting values are: $\omega_r=0.003\ 86$ kHz, $NU_0=26.604$ kHz, and $NU_2=0.123\ 66$ kHz. This completely fixes from a microscopic level the parameters used in the two-mode description.

First let us consider the simplest full GP simulation, listed as I in Table I. This consists of the three components starting from the same initial population imbalances and basically gives a similar Josephson tunneling behavior for the three components. As can be seen in Fig. 1 the Josephson regime is fully identified on the coupled behavior of z_m and $\delta\phi_m$. Together with the Josephson oscillation there is a transfer of population between the three different states, see panel (b) of Fig. 1. As discussed above the population transfer dynamics decouples from the Josephson tunneling in this regime and thus allows to clearly identify the value of NU_2, which is of course directly linked to c_2. The agreement between the two-mode and the full GP simulation is remarkable as can be seen in Fig. 1. Taking into account that for ^{87}Rb $|c_2|\ll c_0$ and therefore $U_2N\ll U_0N$, it is easy to prove from the above two-mode equations that, for this case, the behavior of the imbalance of all the components follows: $\ddot{z}_m=-\omega_T^2z_m$ with

TABLE I. Conditions of the different full spinor GP simulations, Eq. (1). $\delta\phi_m(0)=0$ in all cases.

Sim	$N_0(0)/N$	$z_{-1}(0)$	$z_0(0)$	$z_{+1}(0)$	Transfer
I	0.4	0.005	0.005	0.005	Yes
IIa(b)	0.6	0.010	0.000	0.020	Yes(no)
IIIa(b)	0.6	0.000	0.010	0.000	Yes(no)
IVa(b)	0.6	0.010	0.000	−0.010	Yes(no)

$\omega_J=\omega_r\sqrt{1+NU_0/\omega_r}$, which corresponds to the Josephson frequency of a scalar condensate completely decoupled from the population transfer [7]. Therefore, the Josephson tunneling is directly related to the spin independent coupling, proportional to U_0.

Now we consider three distinct cases: IIa, IIIa, and IVa. As listed in Table I they correspond to different initial population imbalances for the three components and to a different initial number of atoms populating each sublevel from the one used in I. In Fig. 2 we show the results of the full GP simulations (solid lines). Runs IIa and IIIa produce essentially Josephson tunneling dynamics modulated by a longer oscillation. Simulation IVa, produces a much longer tunneling, the ±1 components remain mostly on their original side of the trap while the 0 one remains mostly balanced. In the first two cases the oscillations of the phase differences are fully characterized by ω_J. In the same figure, and almost indistinguishable from the full GP results, we present the predictions of the two-mode model.

As mentioned above the population transfer dynamics fully decouples from the Josephson tunneling of the three components in the considered conditions. Its counterpart is however not true, the Josephson dynamics gets affected by the population transfer as we will discuss in the following.

To clearly see the effect of the population transfer terms on top of the Josephson tunneling dynamics we consider the same configurations, labeled as "a," but without the population transfer terms, "b." The two-mode model, without the corresponding transfer terms, also reproduces the dynamics of the "b" runs. In Fig. 3 we depict in all cases a comparison between the full GP solution and the same case but neglecting the population transfer term.

The effects of population transfer are clearly seen on the evolution of z_m. In simulation II, which has $z_0(0)=0$ it is observed that the long oscillation which modulates the full runs, ω_T, is not present when we switch off the transfer term. Instead the population imbalance shows a Josephson-like tunneling oscillation which for $t\sim100$ ms looses the small z_m regime. Therefore, the transfer term tends to stabilize the Josephson-like behavior over longer periods of time. The absence of transfer of populations does not show up on the behavior of the phase difference, as can be seen in Fig. 3, which mostly follows the same evolution as for the GP equations with the transfer term.

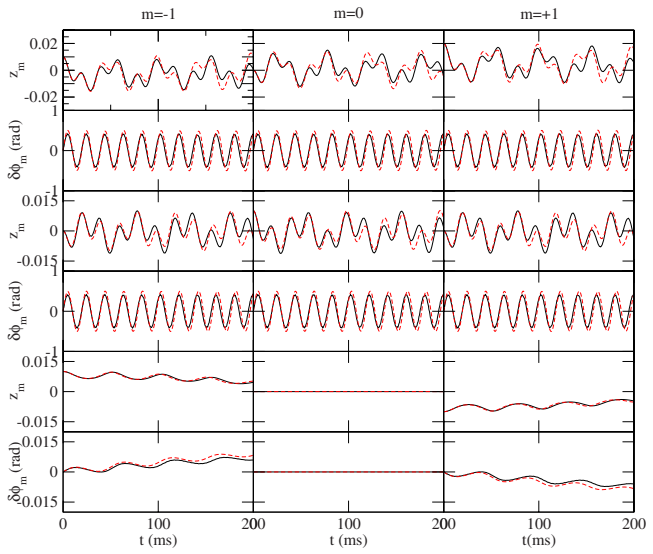

FIG. 2. (Color online) Full simulation of Eq. (1) and two-mode analysis of some cases listed in Table I. The first, second; third, fourth; and fifth, sixth rows correspond to simulations IIa, IIIa, and IVa, respectively. Solid lines correspond to the GP simulations. Dashed lines depict two-mode results with the parameters computed microscopically as described in the text. In most cases the two lines in each panel are almost indistinguishable.

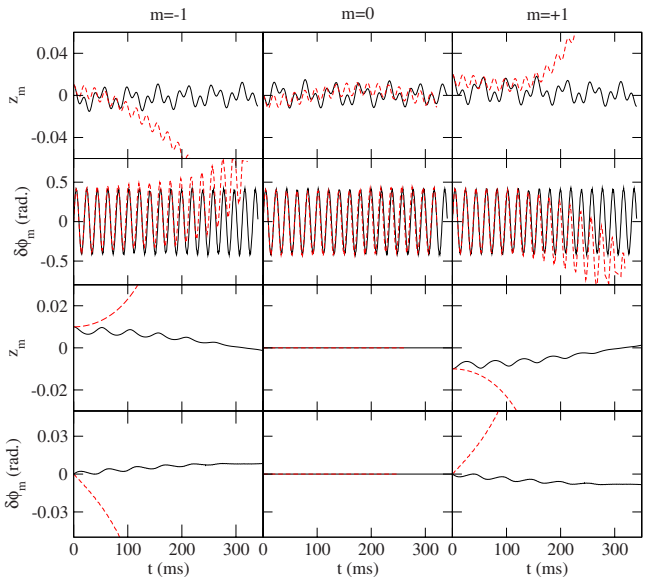

FIG. 3. (Color online) The first, second, and third, fourth rows correspond to simulations IIa(b) and IVa(b) described in Table I. Solid (black) lines correspond to IIa and IVa while dashed (red) lines stand for IIb and IVb, which do not include the population transfer terms.

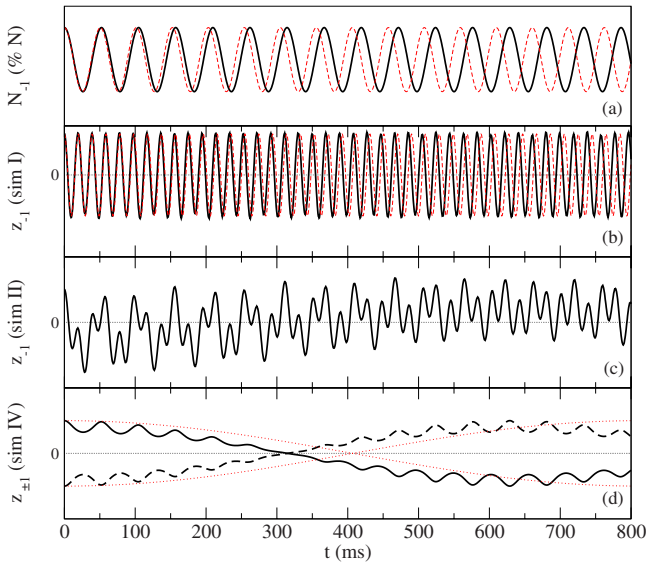

FIG. 4. (Color online) Figure which shows the frequencies entering in the problem. (a) Time evolution of the number of atoms populating the $m=-1$ sublevel in simulation I, solid line. The dashed line depicts a $\cos(\omega_T t)$ which is the two-mode prediction for $N_0 \sim N/2$. (b) Full GP evolution for z_{-1} of simulation I, solid line. The dashed line shows a $\cos(\omega_J t)$ behavior, clearly identifying the Josephson time scale. (c) Full GP evolution of z_{-1} for simulation II. The dynamics is governed by (ω_T, ω_J). (d) The solid black (red-dashed) line corresponds to the GP evolution of z_{-1} (z_{+1}) of simulation IV. The dotted lines follow a $\cos(\omega_r t)$, which drives the long-time scale of the problem. The scales in the vertical axes are not shown for clarity.

As in the case of binary mixtures [16], taking opposite initial imbalances for the $m=\pm 1$ components enhances the Rabi like oscillation and cancels the Josephson one. Simulation IV corresponds to such a case, with $z_{-1}(0)=-z_{+1}(0)$ and $z_0(0)=0$. The Rabi oscillation gives rise to a long tunneling behavior but in this case modulated by the ω_T oscillation, as can be seen in Fig. 3 and in the lowest panel of Fig. 4. If we switch off the transfer term the ω_T oscillation disappears and the limit of small z and $\delta\phi$ becomes unstable.

Finally, Fig. 4 summarizes the relevant frequencies which enter in the interplay between Josephson tunneling and population transfer dynamics in the considered regime. The first panel isolates $\omega_T = NU_2$, governing the transfer of populations, whereas the second one shows ω_J, which sets the fast behavior of the imbalances. The third panel shows z_{-1} from simulation II, which is dominated by (ω_T, ω_J) and the fourth one shows both $z_{\pm 1}$ from simulation IV, that are dominated by two frequencies (ω_T, ω_r).

The ability to perform an experiment with spinor $F=1$ BEC in the conditions considered in this work would present the combined effects of Josephson tunneling phenomena and the transfer of population between different Zeeman components of a spinor condensate: the decoupling of the exchange of populations from the Josephson dynamics, the identification of the different time scales and the role of the population transfer in the stability of the Josephson oscillations. In addition, a precise measurement of the population imbalances and global populations of the three species would provide an alternative access to the microscopic properties of the atom-atom interactions.

We thank Joan Martorell and Maciej Lewenstein for a careful reading of the manuscript and motivating discussions. B.J.-D. is supported by a CPAN CSD (Contract No. 2007-0042) contract, Consolider Ingenio 2010. This work is also supported Generalitat de Catalunya (Grants No. FIS2008-01661, No. FIS2008-00421, and No. 2009SGR-1289).

[1] M. S. Chang *et al.*, Nat. Phys. **1**, 111 (2005).
[2] M. S. Chang, C. D. Hamley, M. D. Barrett, J. A. Sauer, K. M. Fortier, W. Zhang, L. You, and M. S. Chapman, Phys. Rev. Lett. **92**, 140403 (2004).
[3] M. Lewenstein *et al.*, Adv. Phys. **56**, 243 (2007).
[4] C. Orzel *et al.*, Science **291**, 2386 (2001).
[5] M. Albiez, R. Gati, J. Folling, S. Hunsmann, M. Cristiani, and M. K. Oberthaler, Phys. Rev. Lett. **95**, 010402 (2005).
[6] R. Gati and M. K. Oberthaler, J. Phys. B **40**, R61 (2007).
[7] A. Smerzi, S. Fantoni, S. Giovanazzi, and S. R. Shenoy, Phys. Rev. Lett. **79**, 4950 (1997).
[8] Q. Niu, X.-G. Zhao, G. A. Georgakis, and M. G. Raizen, Phys. Rev. Lett. **76**, 4504 (1996); S. R. Wilkinson, C. F. Bharucha, K. W. Madison, Q. Niu, and M. G. Raizen, *ibid.* **76**, 4512 (1996); M. Ben Dahan, E. Peik, J. Reichel, Y. Castin, and C. Salomon, *ibid.* **76**, 4508 (1996); D. L. Haycock, P. M. Alsing, I. H. Deutsch, J. Grondalski, and P. S. Jessen, *ibid.* **85**, 3365 (2000).
[9] D. Ananikian and T. Bergeman, Phys. Rev. A **73**, 013604 (2006).
[10] T.-L. Ho, Phys. Rev. Lett. **81**, 742 (1998); T. Ohmi and K. Machida, J. Phys. Soc. Jpn. **67**, 1822 (1998).
[11] H. Pu, W. P. Zhang, and P. Meystre, Phys. Rev. Lett. **89**, 090401 (2002); Ö. E. Müstecaplioglu, W. Zhang, and L. You, Phys. Rev. A **75**, 023605 (2007).
[12] E. M. Chudnovsky and J. Tejada, *Cambridge Studies in Magnetism* (CUP, Cambridge, 1998), Vol. 4.
[13] E. G. M. van Kempen, S. J. J. M. F. Kokkelmans, D. J. Heinzen, and B. J. Verhaar, Phys. Rev. Lett. **88**, 093201 (2002).
[14] M. Moreno-Cardoner, J. Mur-Petit, M. Guilleumas, A. Polls, A. Sanpera, and M. Lewenstein, Phys. Rev. Lett. **99**, 020404 (2007).
[15] S. Ashhab and C. Lobo, Phys. Rev. A **66**, 013609 (2002); H. T. Ng, C. K. Law, and P. T. Leung, *ibid.* **68**, 013604 (2003); L. Wen and J. Li, Phys. Lett. A **369**, 307 (2007); I. I. Satija, R. Balakrishnan, P. Naudus, J. Heward, M. Edwards, and C. W. Clark, Phys. Rev. A **79**, 033616 (2009).
[16] B. Juliá-Díaz, M. Guilleumas, M. Lewenstein, A. Polls, and A. Sanpera, Phys. Rev. A **80**, 023616 (2009).